JOURNAL OF AGRICULTURAL AND FOOD CHEMISTRY

Cytotoxic Effects of New Geranyl Chalcone Derivatives Isolated from the Leaves of *Artocarpus communis* in SW 872 Human Liposarcoma Cells

SONG-CHWAN FANG,[†] CHIN-LIN HSU,[‡] YU-SHEN YU,[‡] AND GOW-CHIN YEN*[,‡]

Department of Food Nutrition, Chung Hwa University of Medical Technology, 89 Wenhwa First Street, Tainan 71703, Taiwan, and Department of Food Science and Biotechnology, National Chung Hsing University, 250 Kuokuang Road, Taichung 40227, Taiwan

Breadfruit (*Artocarpus communis* Moraceae) is cultivated in tropical and subtropical regions as a traditional starch crop and also has potential medicinal properties. The aim of this work was to study the *in vitro* anticancer activity of compounds isolated from the leaves of *Artocarpus communis*. Three new geranyl chalcone derivatives including isolespeol (**1**), 5′-geranyl-2′,4′,4-trihydroxychalcone (**2**), and 3,4,2′,4′-tetrahydroxy-3′-geranyldihydrochalcone (**3**), together with two known compounds lespeol (**4**) and xanthoangelol (**5**), were isolated from the leaves of *Artocarpus communis*. The structures of **1**−**5** were elucidated by spectroscopy and through comparison with data reported in the literature. The effects of geranyl chalcone derivatives (**1**−**5**) on the viability of human cancer cells (including SW 872, HT-29, COLO 205, Hep3B, PLC5, Huh7, and HepG2 cells) were investigated. The results indicate that isolespeol (**1**) showed the highest inhibitory activity with an IC_{50} value of 3.8 μM in SW 872 human liposarcoma cells. Treatment of SW 872 human liposarcoma cells with isolespeol (**1**) caused the loss of mitochondrial membrane potential ($\Delta\Psi$m). Western blotting revealed that isolespeol (**1**) stimulated increased protein expression of Fas, FasL, and p53. The expression ratios of pro- and antiapoptotic Bcl-2 family members were also changed by isolespeol (**1**) treatment to subsequently induce the activation of caspase-9 and caspase-3, which was followed by cleavage of poly (ADP-ribose) polymerase (PARP). These results demonstrate that isolespeol (**1**) induces apoptosis in SW 872 cells through Fas- and mitochondria-mediated pathways.

KEYWORDS: ***Artocarpus communis*; cancer; apoptosis; isolespeol**

INTRODUCTION

Uncontrolled cell growth is observed in several human diseases including cancer. The control of cancer cell growth by inhibition of the cell cycle and induction of apoptosis could provide a therapeutic strategy for the treatment of cancer (*1*). Apoptosis or programmed cell death plays an important role in the regulation of cellular homeostasis (*2*). Apoptosis is characterized by the activation of the caspase family of cysteine proteases, followed by caspase-mediated specific morphological changes including cell shrinkage, chromatin condensation, nuclear DNA fragmentation, membrane blebbing, and breakdown of the cell into apoptotic bodies (*3*). In cells responsive to apoptotic stimuli, there are two major apoptotic pathways that involve intrinsic and extrinsic signaling. These may be initiated through the regulation of death receptors located on the cell surface or through an intrinsic pathway that relies on the release of apoptotic signals from mitochondria (*4*). Many models of apoptosis show a loss of the mitochondrial membrane potential ($\Delta\Psi$m) mediated by opening of megachannels (permeability transition pores), which precedes caspase activation (*5*).

Small molecular compounds isolated from plants have been widely investigated for many medical applications including cancer prevention and control (*6*). Breadfruit (*Artocarpus communis* Moraceae) is cultivated in tropical and subtropical regions for its leaves. Breadfruit is also a traditional starch crop in Oceania regions such as Melanesia, Micronesia, and Polynesia (*7*). Its roots have been used in traditional medicine as an antiphlogistic, diuretic, and expectorant; it is used to treat headache, beriberi, vomiting, parulis, and dropsy (*8, 9*). *Artocarpus* species, a rich source of prenylated flavonoids and their derivatives, have been investigated phytochemically and biologically for antifungal, radical scavenging, anti-inflammatory, and antiplatelet activities (*10*−*15*). Some studies have indicated that prenylated flavonoids from *Artocarpus communis* inhibit nitric oxide production in LPS-stimulated RAW 264.7 cells (*12, 13*). Breadfruit (*Artocarpus communis*) seeds have been described as containing two α-mannosidases and have several applications in the food and biotechnology industry (*16*). Adewole and Ojewole (*17*) indicated that water extract of *Artocarpus com-*

* To whom correspondence should be addressed. Tel: 886-4-2287-9755. Fax: 886-4-2285-4378. E-mail: gcyen@nchu.edu.tw.
[†] Chung Hwa University of Medical Technology.
[‡] National Chung Hsing University.

10.1021/jf8017436 CCC: $40.75
Published on Web 09/04/2008

munis root induced acute hyperglycaemia in Wistar rats. However, literature demonstrating the anticancer activity of geranyl chalcone derivatives isolated and identified from the leaves of *Artocarpus communis* remains scarce.

The objective of this study was to investigate the anticancer activity of geranyl chalcone derivatives isolated and identified from the leaves of *Artocarpus communis*. In the present study, various human cancer cells (including SW 872, HT-29, COLO 205, Hep3B, PLC5, Huh7, and HepG2 cells) were used for *in vitro* evaluation of anticancer activity. The apoptotic effects of compounds isolated from the leaves of *Artocarpus communis* on Fas- and mitochondria-mediated pathways in human cancer cells were investigated.

MATERIALS AND METHODS

Materials. Leaves of *Artocarpus communis* were collected at Tainan Hsien, Taiwan, in November 2005. Sodium bicarbonate, MTT dye [3-(4,5-dimethylthiazol-2-yl)-2,5-diphenyl tetrazolium bromide], propidium iodide (PI), and 4,6-diamidino-2-phenylindole dihydrochloride (DAPI) were purchased from Sigma Chemical Co. (St. Louis, MO). Dimethylsulfoxide (DMSO) was purchased from Merck Co. (Darmstadt, Germany). Dulbecco's modified Eagle's medium, RPMI 1640 medium, Leibovitz's L-15 medium, fetal bovine serum, L-glutamine, nonessential amino acids, sodium pyruvate, and the antibiotic mixture (penicillin−streptomycin) were purchased from Invitrogen Co. (Carlsbad, CA). Anti-β-Actin, anti-Bad, anti-Bak, anti-Bax, anti-Bcl-2, anticaspase-3, anti-Fas, anti-FasL, anti-PARP [poly-(ADP-ribose) polymerase], and anti-p53 antibodies were purchased from Cell Signaling Technology (Beverly, MA). Anti-Bcl-X_L and anti-Bid antibodies were purchased from Biosource (Camarillo, California, USA). The anticaspase-9 antibody was obtained from BioVision (Mountain View, CA). Antirabbit and antimouse secondary horseradish peroxidase antibodies were purchased from Bethyl Laboratories (Montgomery, TX). Protein molecular mass markers were obtained from Pharmacia Biotech (Saclay, France). Polyvinyldifluoride (PVDF) membranes for Western blotting were obtained from Millipore (Bedford, MA). All other chemicals were reagent grade.

Extraction and Isolation of Geranyl Chalcone Derivatives from the Leaves of *Artocarpus communis*. Dried ground leaves (3.2 kg) were extracted with methanol (20 L) two times in a percolator and filtered. The filtrate was evaporated in vacuo to produce a dark brown residue, which was suspended in water and partitioned with dichloromethane. The dichloromethane extract (53.5 g) was chromatographed on silica gel (70−230 mesh, 1.8 kg, Merck) with step gradients in an *n*-C_6H_{14}-EtOAc solvent system (100:0, 9:1, 7:1, 5:1, 2:1, 1:1, 0:100, v/v, each step containing 2.5 L) to give fractions A−E in the TLC profile. Fraction A (*n*-C_6H_{14}-EtOAc, 9:1−7:1, 6.8 g) was further fractionated using silica gel column chromatography (70−230 mesh, 162 g, Merck) and eluted with an *n*-C_6H_{14}-EtOAc solvent system (10:1, 8:1, 5:1, 2:1, 1:1, 0:1, v/v, each step containing 800 mL) to yield 15 fractions. These fractions (*n*-C_6H_{14}-EtOAc, 8:1−5:1, fraction 4−6) were rechromatographed on silica gel (230−400 mesh, 63 g, Merck) and eluted with C_6H_6-EtOAc (6:1, v/v) to provide 5 fractions. Fraction 4 was purified by preparative TLC and developed with CH_2Cl_2-EtOAc (10:1, v/v) to obtain isolespeol (**1**, 16.8 mg), and 2′,4′,4-trihydroxy-5′-geranylchalcone (**2**, 18.5 mg). Fraction C (*n*-C_6H_{14}-EtOAc, 5:1−2:1, 4.2 g) was rechromatographed on a silica gel (230−400 mesh, 132 g, Merck) by eluting with C_6H_6-EtOAc (4:1, v/v) to provide fractions 1−8 by TLC profile. Purification of fractions 3 and 5 by preparative silica gel TLC with CH_2Cl_2-EtOAc (8:1 and 6:1, v/v, respectively) provided two known compounds: lespeol (**4**, 6.2 mg) and xanthoangelol (**5**, 22.4 mg). TLC was performed in C_6H_6-CH_2Cl_2-EtOAc (1:1:0.6) to obtain 3,4,2′,4′-tetrahydroxy-3′-geranyldihydrochalcone (**3**, 12.6 mg).

Spectrometry. Optical rotations were measured with a JASCO DIP-370 digital polarimeter (JASCO, Tokyo, Japan). UV spectra were obtained on a Thermo model α UV/vis spectrophotometer (Thermo Spectronic, Cambridge, England). IR spectra were recorded on a Perkin-Elmer 2000 FT-IR spectrophotometer (Fremont, CA, USA). ^{1}H (400 MHz) and ^{13}C NMR (100 MHz) experiments were performed with a Varian Unity 400 NMR spectrophotometer (Varian, CA, USA). MS data were obtained on a JMS HX-100 mass spectrometer (JEOL Ltd., Tokyo, Japan).

Table 1. ^{13}C NMR Data of Compounds **1**−**5** in $CDCl_3$ (100 M H_2)

carbon number	1	2	4	5	carbon number	3
1	127.6	127.7	127.5	127.7	1	134.0
2	130.6	130.6	130.6	130.6	2	115.5
3	116.0	116.0	116.0	116.0	3	141.9
4	158.1	158.0	158.2	158.0	4	143.6
5	116.0	116.0	116.0	116.0	5	115.4
6	130.6	130.6	130.6	130.6	6	120.7
β	144.1	144.2	144.2	144.1	1′	113.9
α	117.8	117.9	117.7	118.0	2′	162.6
C=O	191.7	192.0	192.1	192.2	3′	113.3
1′	114.0	114.3	113.9	114.0	4′	161.7
2′	161.0	161.8	160.2	161.8	5′	108.0
3′	104.4	104.1	109.2	114.0	6′	129.5
4′	166.6	164.9	160.8	163.8	7′	204.0
5′	113.4	118.8	108.1	107.9	8′	39.8
6′	127.4	131.0	130.7	129.2	9′	29.9
1″	121.7	29.1	127.0	21.7	1″	21.6
2″	127.7	121.4	116.3	121.0	2″	120.9
3″	80.5	139.3	80.3	139.8	3″	139.7
4″	41.9	39.7	41.6	39.7	4″	39.7
5″	22.6	26.6	27.2	26.3	5″	26.3
6″	123.7	123.6	123.8	123.7	6″	123.7
7″	132.0	132.2	131.9	132.1	7″	132.1
8″	25.6	25.7	25.7	25.7	8″	25.6
9″	27.5	17.7	22.6	17.7	9″	17.7
10″	17.6	16.3	17.6	16.3	10″	16.2

Table 2. Effect of Compounds **1**−**5** on Viability in Human Cancer Cells

	IC_{50} (μM)[a]			
cell line	1	2	3	5
SW 872	3.8 ± 0.2	4.1 ± 0.7	4.3 ± 0.8	4.4 ± 0.4
HT-29	11.0 ± 1.1	11.6 ± 0.9	19.7 ± 3.5	16.3 ± 0.5
COLO 205	16.3 ± 0.8	[b]	12.6 ± 0.3	12.0 ± 1.1
Hep3B	17.1 ± 0.2	4.0 ± 0.1	13.8 ± 1.2	6.0 ± 0.4
PLC5	8.6 ± 0.0	8.7 ± 0.2		11.0 ± 0.7
Huh7	17.6 ± 0.0	9.0 ± 0.3		9.5 ± 0.0
HepG2		22.1 ± 0.3		18.3 ± 0.4

[a] Cells were treated with 0−25 μM of compounds **1**−**5** for 48 h. [b] The IC_{50} value was over 25 μM. The reported values are the means ± SD (n = 4).

Compound **1** was named isolespeol. Its chemical and physical properties were as follows: orange-yellow gum; $[\alpha]_D$ +21° ($CHCl_3$, c 0.12); UV (MeOH) λmax (log ε): 226 (4.39), 276 (4.35), 370 (4.19) nm; IR $\nu CHCl_3$ max cm^{-1}: 3285, 1634, 1607, 1560; ^{1}H NMR (400 MHz, $CDCl_3$): σ1.43 (3H, s, H-10″), 1.57 (3H, s, H-8″), 1.66 (3H, s, H-9), 1.68 (1H, m, H_α-4″), 1.75 (1H, m, H_β-4″), 2.09 (2H, m, H-5″), 5.08 (1H, m, H-6″), 5.53 (1H, d, J = 10.4 Hz, H-2″), 6.37 (1H, d, J = 10.4 Hz, H-1″), 6.37 (1H, s, H-3′), 6.89 (2H, d, J = 8.8 Hz, H-3 and H-5), 7.42 (1H, d, J = 15.2 Hz, H-α), 7.48 (1H, s, H-6′), 7.57 (2H, d, J = 8.8 Hz, H-2 and H-6), 7.83 (1H, d, J = 15.2 Hz, H-β), 13.56 (1H, s, OH); for ^{13}C NMR spectrum (100 MHz, $CDCl_3$), see **Table 1**; EIMS (70ev) m/z (rel. int.): 390 (14), 307 (100), 187 (39). HR-EIMS, m/z $[M]^+$ 390.1831 (calcd for $C_{25}H_{26}O_4$ 390.1831).

Compound **2** was named 2′,4′,4-trihydroxy-5′-geranylchalcone. Its chemical and physical properties were follows: yellow powder; UV (MeOH) λmax (log ε): 229 (sh) (4.33), 292 (4.01), 366 (3.99) nm; IR$\nu CHCl_3$ max cm^{-1}: 3338, 1635, 1604, 1545; ^{1}H NMR (400 MHz, $CDCl_3$): σ1.60 (3H, s, H-9″), 1.68 (3H, s, H-8″), 1.79 (3H, s, H-10″), 2.10 (2H, m, H-4″), 2.15 (2H, m, H-5″), 3.36 (2H, d, J = 7.2 Hz, H-1″), 5.09 (1H, t, J = 6.8 Hz, H-6″), 5.33 (1H, t, J = 7.2 Hz, H-2″), 6.42 (1H, s, H-3′), 6.88 (2H, d, J = 8.4 Hz, H-3 and H-5), 7.43 (1H, d, J = 15.2 Hz, H-α), 7.56 (2H, d, J = 8.4 Hz, H-2 and H-6), 7.63 (1H, s, H-6′), 7.83 (1H, d, J = 15.2 Hz, H-β), 13.31 (1H, s, OH); for ^{13}C NMR spectrum (100 MHz, $CDCl_3$), see **Table 1**; EIMS (70ev)

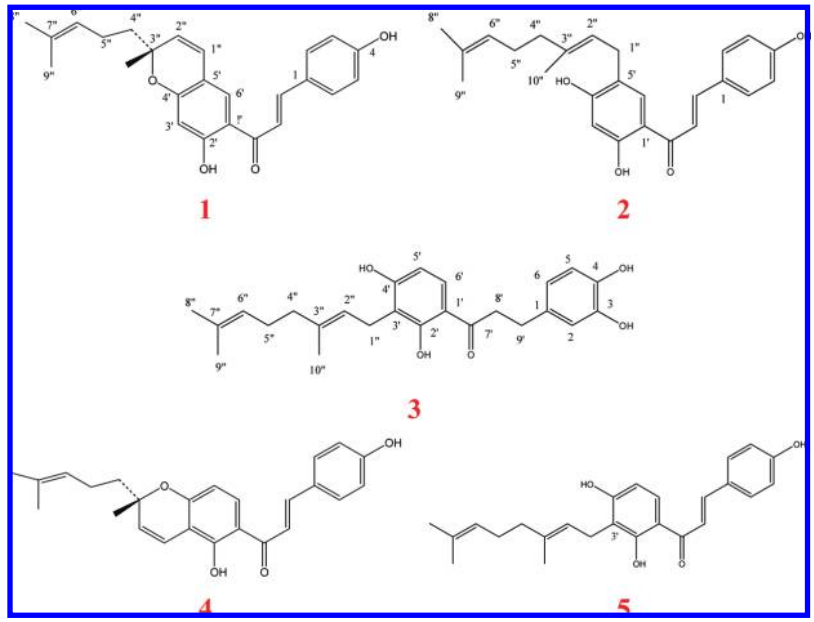

Figure 1. Chemical structure of compounds **1**−**5**.

m/*z* (rel. int.): 392 (85), 323 (36), 307 (32), 269 (100), 203 (69), 161 (36), 149 (74), 147 (89), 123 (45), 120 (63), 107 (31), 91 (78). HR-EIMS, *m*/*z* $[M]^+$ 392.1989 (calcd for $C_{25}H_{28}O_4$ 392.1988).

Compound **3** was named 3,4,2′,4′-tetrahydroxy-3′-geranyldihydrochalcone. Its chemical and physical properties were as follows: yellow gum; UV (MeOH) λmax (log ε): 224 (sh) (4.70), 280 (4.45) nm; IR$\nu$$CHCl_3$ max cm^{-1}: 3378, 1618, 1520, 1496; ^{1}H NMR (400 MHz, $CDCl_3$): σ1.59 (3H, s, H-9″), 1.67 (3H, s, H-8″), 1.81 (3H, s, H-10″), 2.06 (2H, m, H-4″), 2.10 (2H, m, H-5″), 2.93 (2H, t, J = 7.2 Hz, H-9′), 3.17 (2H, t, J = 7.2 Hz, H-8′), 3.45 (2H, d, J = 6.8 Hz, H-1″), 5.04 (1H, t, J = 8.0 Hz, H-6″), 5.26 (1H, t, J = 6.8 Hz, H-2″), 6.36 (1H, d, J = 8.8 Hz, H-5′), 6.65 (1H, dd, J = 8.0 and 2.0 Hz, H-6), 6.75 (1H, d, J = 2.0 Hz, H-2), 6.78 (1H, d, J = 8.0 Hz, H-5), 7.53 (1H, d, J = 8.8 Hz, H-6′), 13.15 (1H, s, OH); for ^{13}C NMR spectrum (100 MHz, $CDCl_3$), see **Table 1**; EIMS (70ev) *m*/*z* (rel. int.): 410 (52), 287 (33), 219 (31), 165 (17), 149 (22), 123 (100). HR-EIMS, *m*/*z* $[M]^+$ 410.2093 (calcd for $C_{25}H_{30}O_5$ 410.2093).

Cell Culture. Human liposarcoma cells (SW 872) and human hepatoblastoma cells (HepG2 and Hep3B) were obtained from the Bioresource Collection and Research Center (BCRC, Food Industry Research and Development Institute, Hsinchu, Taiwan). Human colorectal carcinoma cells (COLO 205 and HT-29) were provided by Dr. Min-Hsiung Pan (National Kaohsiung Marine University, Kaohsiung, Taiwan). Human hepatocellular carcinoma cells (PLC5 and Huh7) were obtained from the American type Culture Collection (ATCC, Bethesda, MD, USA). SW 872 cells were grown in 90% Leibovitz's L-15 medium supplemented with 10% fetal bovine serum, 100 units/mL penicillin, and 100 μg/mL streptomycin. HepG2, Hep3B, PLC5, and Huh7 cells were grown in 90% Dulbecco's modified Eagle's medium supplemented with 10% fetal bovine serum, 2 mM L-glutamine, 1.5 g/L sodium bicarbonate, 0.1 mM nonessential amino acids, 1.0 mM sodium pyruvate, 100 units/mL penicillin, and 100 μg/mL streptomycin. COLO 205 and HT-29 cells were grown in 90% RPMI 1640 medium supplemented with 10% fetal bovine serum, 100 units/mL penicillin, and 100 μg/mL streptomycin. SW 872 cells were cultured at 37 °C in a humidified atmosphere with free gas exchange without CO_2. Other cells were cultured at 37 °C in a humidified 5% CO_2 incubator.

Cell Viability by MTT Assay. The MTT assay was performed according to the method of Mosmann (*18*). Cancer cells were plated into 96-well microtiter plates at a density of 1×10^4 cells/well. After 24 h, the culture medium was replaced by 200 μL serial dilutions (0−100 μM) of compounds **1**−**5**, and cells were incubated for 72 h. The final concentration of solvent was less than 0.1% in the cell culture medium. Culture medium was removed and replaced by 90 μL fresh culture medium. Ten microliters of sterile filtered MTT solution (5 mg/mL) in phosphate buffered saline (PBS, pH 7.4) was added to each well to reach a final concentration of 0.5 mg MTT/mL. After 5 h, unreacted dye was removed, and insoluble formazan crystals were dissolved in 200 μL/well DMSO and measured spectrophotometrically in a FLUOstar galaxy spectrophotometer (BMG Labtechnologies Ltd., Offenburg, Germany) at 570 nm. The relative cell viability (%) as compared to control wells containing cell culture medium without samples was calculated by $A_{570\ nm}$ [sample]/$A_{570\ nm}$ [control] × 100. The IC_{50} value was calculated as the concentration of compounds **1**, **2**, **3**, and **5** under which 50% inhibition of cell growth occurred compared to nontreated controls.

Nuclear Staining with PI and DAPI. Apoptosis was evaluated by staining with PI and DAPI. Cells were stimulated with 0−10 μg/mL isolespeol (**1**) for 48 h. For PI staining, cells were fixed with 80% ethanol for 30 min and incubated with 40 μg/mL PI for 30 min in the dark. For DAPI staining, cells were fixed with 4% paraformaldehyde for 30 min and incubated with 1 μg/mL DAPI solution for 30 min in the dark. The nuclear morphology of the cells was examined by fluorescence microscopy (Olympus, Tokyo, Japan). Typical apoptotic changes included chromatin condensation, chromatin compaction along the periphery of the nucleus, and segmentation of the nucleus.

Mitochondrial Membrane Potential ($\Delta\Psi$m) Analysis. Mitochondrial membrane potential was determined using the MitoPT 100 Test Kit (Immunochemistry Technologies, LLC). JC-1 is a cationic dye that exhibits potential-dependent accumulation in mitochondria and with a fluorescence emission shift from green to red. Cells were seeded in 12-well plates. After 24 h, cells were treated with 0−25 μM isolespeol (**1**) for 6 h. Routine passage consisted of rinsing cells in 12-well plates, once with PBS, followed by harvesting with 0.1 mL of TE solution, addition of 1 mL fresh culture medium, and thorough dispersion. The resulting cell suspensions were aliquotted at 1×10^6 cells per eppendorf tube, with each tube containing 1 mL of culture medium. After centrifugation, cells were incubated with 10 μg/mL JC-1 at 37 °C for 15 min in a humidified 5% CO_2 incubator. Cells were collected and washed with 1× assay buffer (MitoPT 100 Test kit). Cells were resuspended in the same solution and analyzed using a FLUOstar galaxy fluorescence plate reader with excitation at 485 nm and emission at 590 nm for red fluorescence. In this assay, apoptotic cells generate lower levels of red fluorescence, and changes in the mitochondrial membrane potential ($\Delta\Psi$m) can be accurately assessed by comparing the red fluorescence of untreated cells with those treated with isolespeol (**1**). The morphology of the cells was examined by fluorescence microscopy (Olympus, Tokyo, Japan).

Western Blot Analysis. Cells (1×10^7 cells/10 cm dish) were incubated with 0−25 μM isolespeol (**1**) for 3 and 6 h. Cells were collected and lysed in ice-cold lysis buffer [20 mM tris-HCl (pH 7.4),

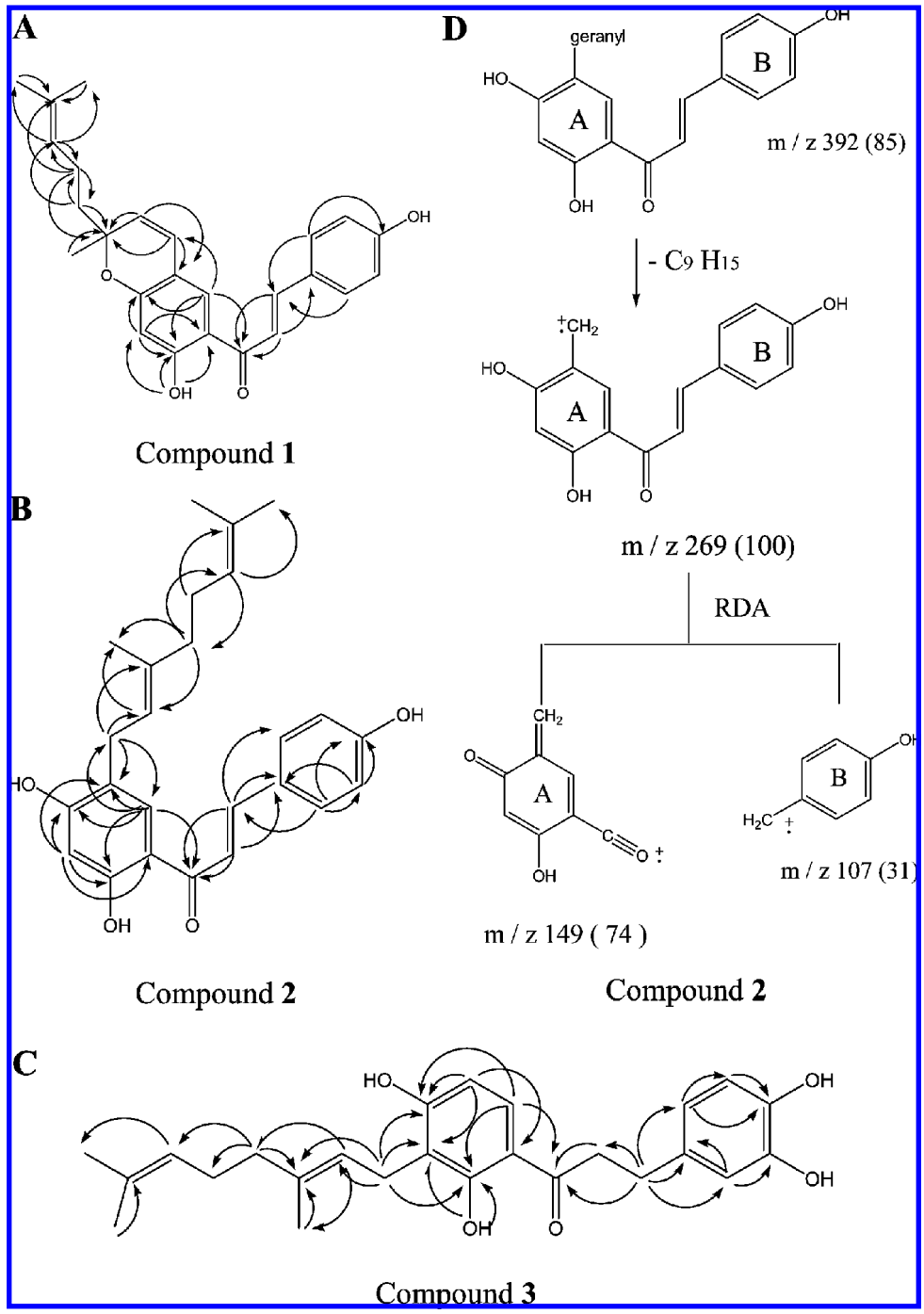

Figure 2. HMBC correlations of compounds **1** (**A**), **2** (**B**), and **3** (**C**), and mass spectral fragmentations of compound **2** (**D**).

2 mM EDTA, 500 μM sodium orthovanadate, 1% Triton X-100, 0.1% SDS, 10 mM NaF, 10 μg/mL leupeptin, and 1 mM PMSF]. Expression of Fas, FasL, p53, Bcl-2, Bax, Bad, Bcl-X_L, Bid, caspase-9, caspase-3, PARP, and β-Actin proteins were assessed in SW 872 cells. The protein concentration of the extracts was estimated with the Bio-Rad DC protein assay (Bio-Rad Laboratories, Hercules, CA, USA) using bovine serum albumin as a standard. Total proteins (50−60 μg) were separated on sodium dodecyl sulfate−polyacrylamide gel electrophoresis (SDS−PAGE) using a 12% polyacrylamide gel. The proteins in the gel were transferred to a PVDF membrane. The membrane was blocked with 5% skim milk in PBST (0.05% v/v Tween-20 in PBS, pH 7.2) for 1 h. Membranes were incubated with primary antibody (1:5000) at 4 °C overnight and then with secondary antibody (1:5000) for 1 h. Membranes were washed three times in PBST for 10 min between each step. Signals were detected using the Amersham ECL system (Amersham-Pharmacia Biotech, Arlington Heights, IL, USA). Relative protein expression was densitometrically quantified using LabWorks 4.5 software and normalized against β-Actin reference bands.

Statistical Analysis. Statistical analysis was performed using SAS software. Analyses of variance was performed using ANOVA. Significant differences ($p < 0.05$) between the means were determined by Duncan's multiple range tests. Each experiment was performed in triplicate.

RESULTS AND DISCUSSION

Isolation and Identification of Geranyl Chalcone Derivatives from the Leaves of *Artocarpus communis*. The CH_2Cl_2-soluble fraction of the leaves of *A. communis* gave rise to five geranyl chalcone derivatives (**Figure 1**). The characteristics of new compounds **1**−**3** were elucidated by spectroscopic data

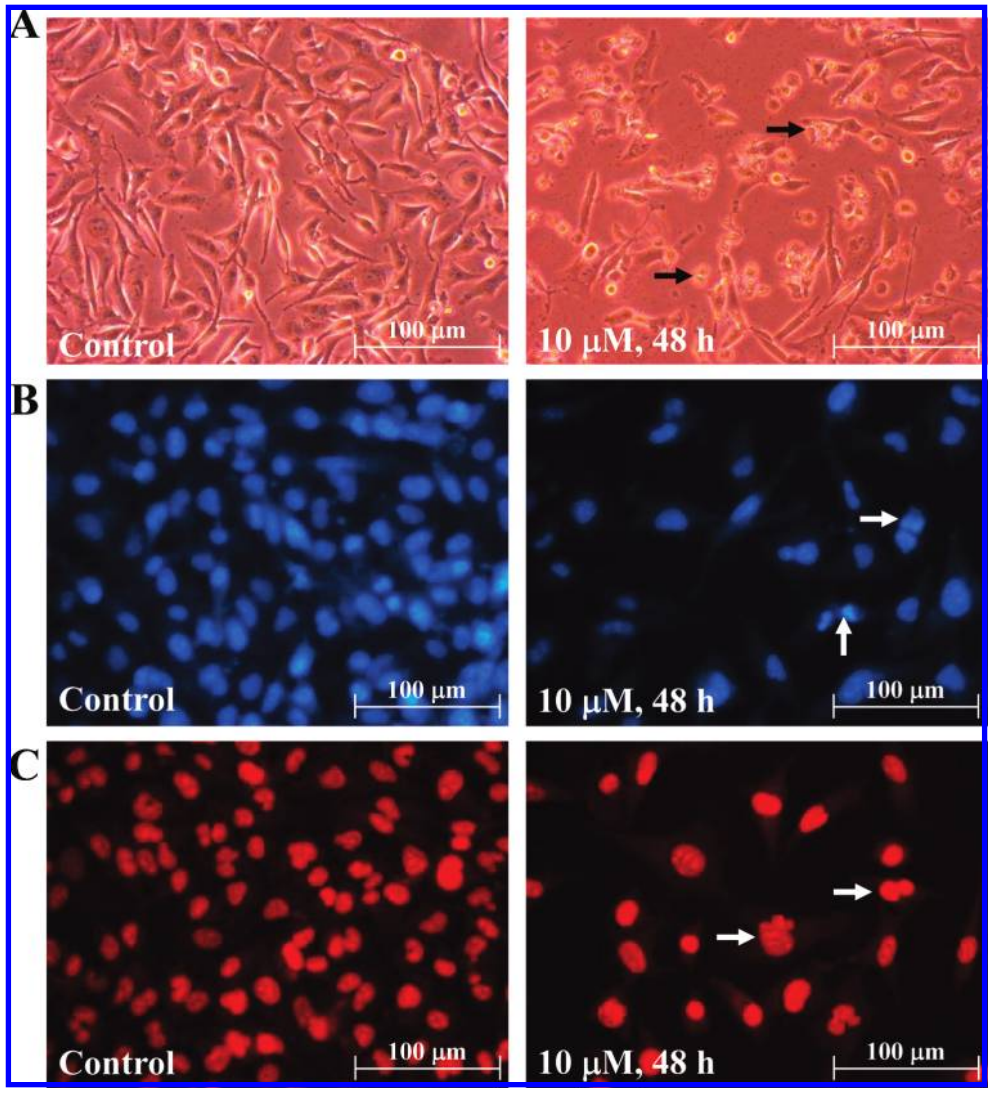

Figure 3. Effect of isolespeol (**1**) on cell morphology in SW 872 human liposarcoma cells. (**A**) Unstained, (**B**) stained with DAPI, and (**C**) stained with PI. Cells were treated with 0−10 μM isolespeol (**1**) for 48 h.

(UV, IR, HREIMS, ^{1}H NMR, ^{1}H−^{1}H COSY, ^{1}H−^{1}H NOESY, ^{13}C NMR, HMBC, and HMQC). Compounds **4** and **5** were identified by comparing their spectroscopic data to previously reported values.

Compound **1** was obtained as an orange−yellow gum. The HREIMS showed a $[M]^+$ peak at *m/z* 390.1831 and corresponded to the molecular formula $C_{25}H_{26}O_4$. The IR spectrum exhibited a hydroxyl group absorption band at ν_{max} 3285 cm^{-1} and a carbonyl group absorption band at ν_{max} 1634 cm^{-1}. The UV spectrum exhibited maxima at 226, 276, and 370 nm, which suggested compound **1** to have a chalcone skeleton (*19*). The ^{1}H NMR spectrum of **1** showed signals for protons at the C-α and C-β positions of the chalcone skeleton [δ 7.42 (1H, d, J = 15.2 Hz), 7.83 (1H, d, J = 15.2 Hz)], as well as A_2B_2-type aromatic protons [δ6.89 (2H, d, J = 8.8 Hz), 7.57 (2H, d, J = 8.8 Hz)], a chelated phenolic proton [δ13.56 (1H, s)], two aromatic protons [δ6.37 (s) and 7.48 (s)], and resonances due to a 2-methyl-2-(4-methylpent-3-enyl) 2*H*-pyran ring [δ1.43, 1.57 and 1.66 (each 3H, s), 1.68 and 1.75 (each 1H, m) assignable to H-4$_\alpha$″ and H-4$_\beta$″, 2.09 (2H, m), 5.08 (1H, m), 5.53 (1H, d, J = 10.4 Hz), 6.37 (1H, d, J = 10.4 Hz)]. ^{1}H−^{1}H NOESY showed cross-peaks between Me-10″/H$_\beta$-4″ and Me-10″/H-2″, confirming that the methyl group was linked at C-3. The ^{1}H−^{1}H COSY correlation of H-4″ to H-5″ and H-5″ to H-6″ as well as the HMBC correlations (**Figure 2A**) of H-4″/C-3″, C-4″, and C-5″; H-5″/C-3″, C-5″ and C-7″; and H-6″/C-5″ and C-8″ confirmed that the 4-methyl-pent-3-enyl group was linked at C-3. ^{1}H−^{1}H NOESY further showed a cross-peak between H-6′/H-1″ and H-1″/H-2″, and the HMBC correlations of H-6′/C-2′, C-4′, C-6′, C-1″, and C═O, and H-1″/C-5′, C-6′, and C-3″ confirmed that the pyran ring was linked at C-4′ and C-5′. The ^{13}C NMR spectrum of **1** showed 25 carbon signals comprising 3 methyls and 2 methylenes, 11 methines, and 8 quaternary carbons, including 1 carbonyl group (δ_C 191.7). On the basis of the above evidence, the structure of isolespeol (**1**) was determined to be a new compound, 2′,4-dihydroxy-4′,5′-[2-methyl-2- (4-methylpent-3-enyl)-pyran]chalcone.

Compound **2** was a yellow powder. The HREIMS exhibited an $[M]^+$ peak at *m/z* 392.1989 and corresponded to the molecular formula $C_{25}H_{28}O_4$. The IR spectrum exhibited a hydroxyl group absorption band at ν_{max} 3338 cm^{-1} and a carbonyl group absorption band at ν_{max} 1635 cm^{-1}. The UV spectrum of **2** exhibited absorption maxima at 229, 292, and 366 nm, which were consistent with those of a chalcone skeleton (*20*). The ^{1}H NMR spectrum of **2** showed a geranyl group [δ1.60, 1.68, and 1.79 (each 3H, s), 2.10 (2H, m), 2.15 (2H, m), 3.36 (2H, d, J = 7.2 Hz), 5.09 (1H, t, J = 6.8 Hz), 5.33 (1H, t, J = 7.2 Hz)], an ortho-coupled aromatic proton at δ6.88 (2H, d, J = 8.4 Hz), 7.56 (2H, d, J = 8.4 Hz) assignable to H-2/H-6 and H-3/H-5, two singlet aromatic protons at δ6.42

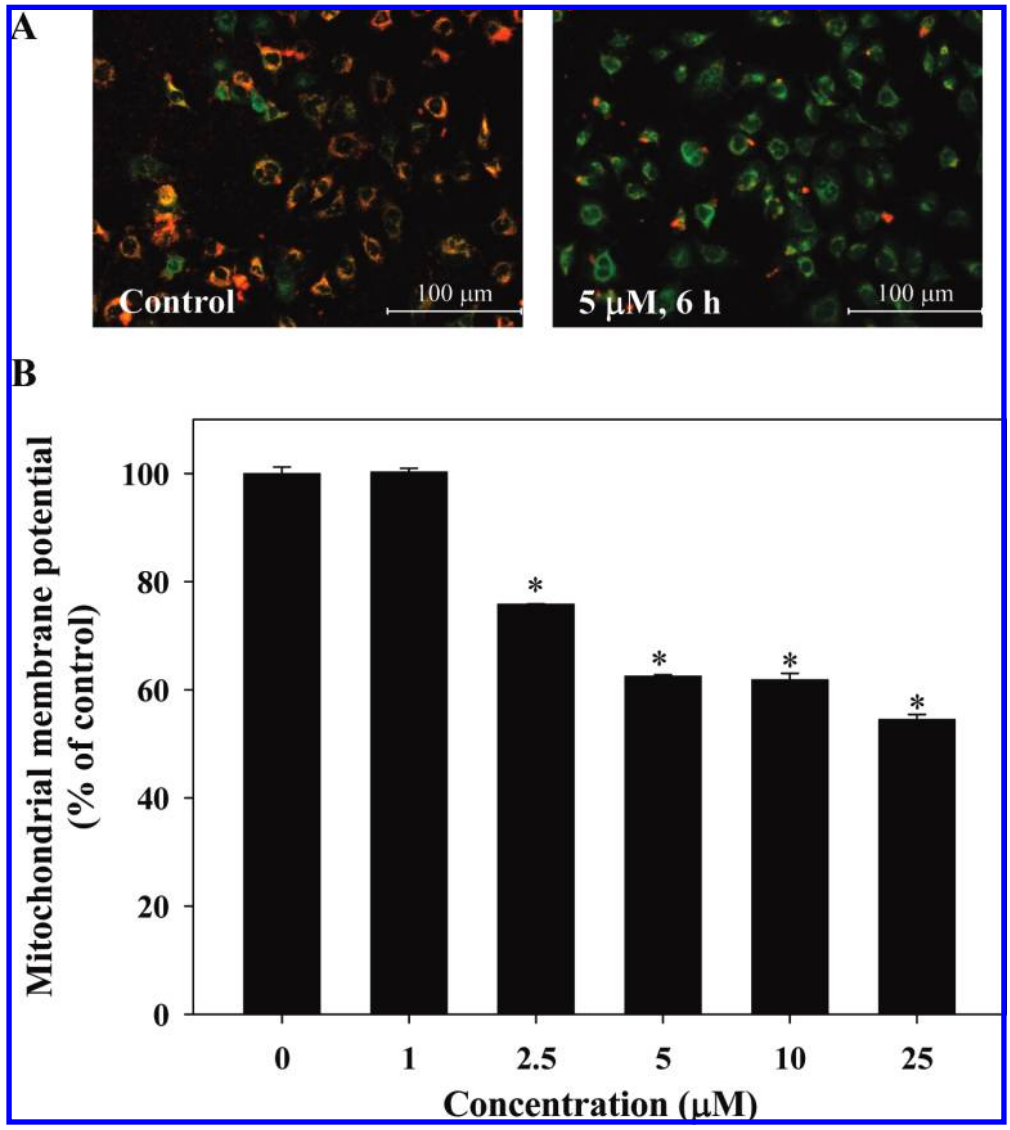

Figure 4. Effect of isolespeol (**1**) on mitochondrial membrane potential ($\Delta\Psi$m) in SW 872 human liposarcoma cells. Cells were treated with 0−25 μM isolespeol (**1**) for 6 h. (**A**) Cells morphological changes. (**B**) Percentages of mitochondrial membrane potential. Results are expressed as percentages of mitochondrial membrane potential as compared with untreated control (mean ± SD, $n = 3$). *Significantly different from control ($p < 0.05$).

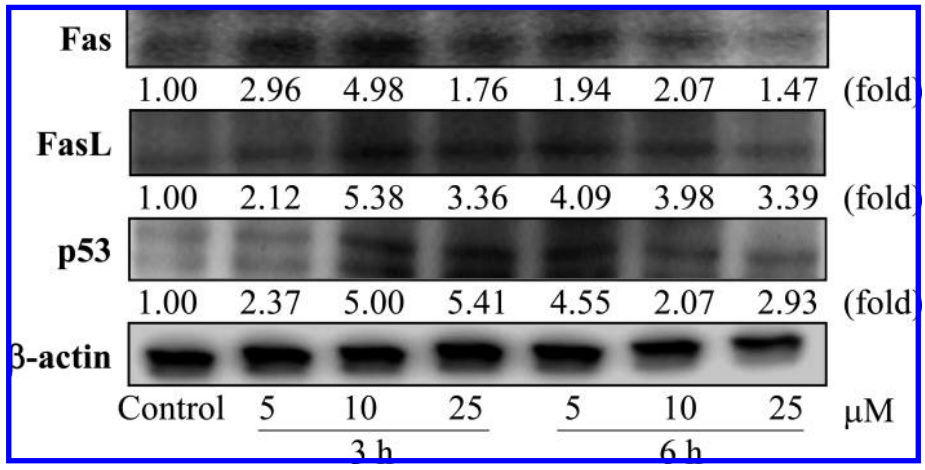

Figure 5. Effect of isolespeol (**1**) on the expression of Fas, Fas-L, and p53 in SW 872 human liposarcoma cells. Cells were treated with 0−25 μM isolespeol (**1**) for 3 and 6 h. Relative protein expression was quantified densitometrically using the LabWorks 4.5 software and normalized against β-Actin reference bands.

and 7.63 assignable to H-3′ and H-6′, and ortho-coupled protons at δ7.43 (1H, d, $J = 15.2$ Hz) and 7.83 (1H, d, $J = 15.2$ Hz) arising from an α,β-unsaturated *trans*-olefin. The low field signal at δ13.31 (1H, s) indicated a C-2′-hydroxy proton intramolecularly hydrogen-bonded to the carbonyl oxygen atom. Geranyl group signals were also implied from the ^{1}H−^{1}H COSY

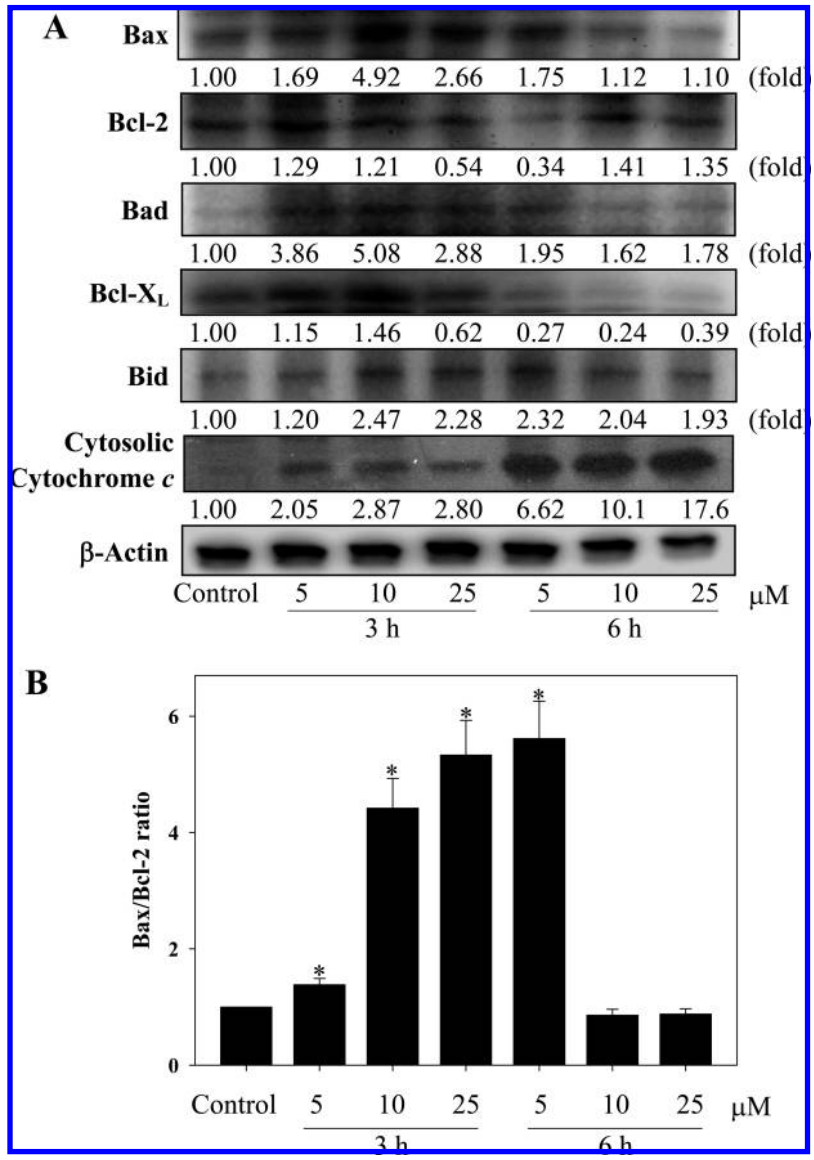

Figure 6. Effect of isolespeol (**1**) on the expression of Bcl-2 family and cytochrome *c* (**A**), and Bax/Bcl-2 ratio (**B**) in SW 872 human liposarcoma cells. Cells were treated with 0−25 μM isolespeol (**1**) for 3 and 6 h. Relative expression was quantified densitometrically using LabWorks 4.5 software and normalized against β-Actin reference bands. Reported values are the means ± SD ($n = 3$). *Significantly different from control ($p < 0.05$).

correlation of H-1″ to H-2″ and H-5″ to H-6. Cross-peaks between H-6′/H-1″ and H-2″ on ^{1}H−^{1}H NOESY as well as the HMBC correlations (**Figure 2B**) of H-6′/C-1″, C-2′, C-4′, C-5′, and C═O; and H-1″/C-5′, C-6′, and C-2″ confirmed that the geranyl group was linked at C-5′. The ^{13}C NMR spectrum of **2** showed 25 carbon signals comprising 3 methyls and methylenes, 10 methines, and 8 quaternary carbons, including 1 carbonyl group (δ_C 192.0). The EIMS fragmentation (**Figure 2D**) showed significant peaks at *m*/*z* 269, 149, and 107, which further supported the attachment of a geranyl group to ring-A. Therefore, the structure of **2** was elucidated to be a new compound, 5′-geranyl-2′,4′,4-trihydroxychalcone (**2**).

Compound **3** was obtained as a yellow gum. The HREIMS exhibited a $[M]^+$ peak at *m*/*z* 410.2093, which corresponded to a molecular formula of $C_{25}H_{30}O_5$. The IR spectrum showed a hydroxyl group absorption band at ν_{max} 3378 cm^{-1} and a carbonyl group absorption band at ν_{max} 1618 cm^{-1}. The UV spectrum of **3** exhibited absorption maxima at 224 and 280 nm. The ^{1}H NMR spectrum of **3** indicated signals for a chelated phenolic proton at δ13.15 (1H, s), ABX-type aromatic protons at δ6.65 (1H, dd, $J = 8.0$ and 2.0 Hz), 6.75 (1H, d, $J = 2.0$ Hz), and 6.78 (1H, d, $J = 8.0$ Hz), one pair of ortho-coupled aromatic protons at δ6.36 (1H, d, $J = 8.8$ Hz) and 7.53 (1H, d, $J = 8.8$ Hz), and two methylene protons at δ2.93 (2H, t, $J = 7.2$ Hz) and 3.17 (2H, t, $J = 7.2$ Hz). The methylene protons were assigned to H-8 and H-9, respectively, as the former showed HMBC correlations (**Figure 2C**) with C-7, C-9, and C-10, and the latter with C-7, C-8, C-10, C-11, and C-15. The ^{1}H NMR spectrum of **3** further showed geranyl groups at δ1.59, 1.67, and 1.81 (each 3H, s), 2.06 and 2.10 (each 2H, m), and 3.45 (2H, d, $J = 7.2$ Hz), 5.04 (1H, t, $J = 8.0$ Hz), and 5.26 (1H, t, $J = 6.8$ Hz). The presence of geranyl groups was evident from the ^{1}H−^{1}H COSY correlations of H-1″ to H-2″; H-4″ to H-5″; and H-6″ to H-5″, in addition to cross-peaks between H-1″/H-10″; H-2″/H-4″ and H-6″/H-8″ on ^{1}H−^{1}H NOESY. The HMBC correlation data, particularly among H-1″/C-2′, C-3′, C-4′, C-2″, and C-3″ as well as H-5′/C-1′, C-3′, and C-4′; H-6′/C-2′, C-4′, and C-7′, established that the geranyl was located at C-3′. The ^{13}C NMR spectrum of **3** showed 25 carbon signals comprising three methyls, five methylenes, seven methines, and nine quaternary carbons, including one carbonyl (δ204.0).

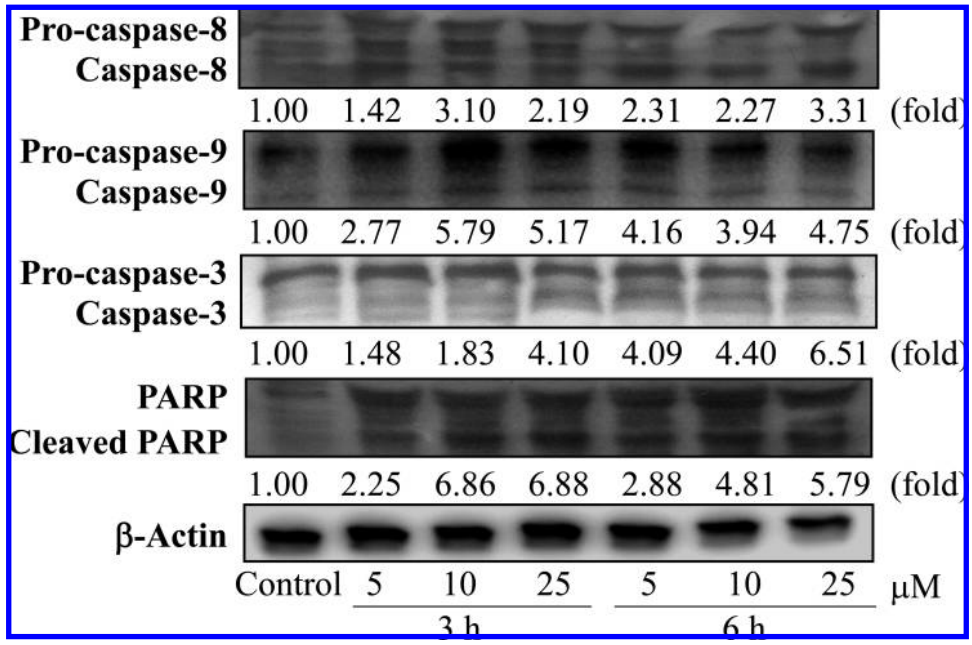

Figure 7. Effect of isolespeol (**1**) on the expression of caspase-8, caspase-9, caspase-3, and PARP in SW 872 human liposarcoma cells. Cells were treated with 0−25 μM isolespeol (**1**) for 3 and 6 h. Reported values are the means ± SD ($n = 3$). Relative protein expression was quantified densitometrically using LabWorks 4.5 software and normalized against β-Actin reference bands. *Significantly different from control ($p < 0.05$).

Therefore, compound **3** was characterized to be a new compound, 3,4,2′,4′-tetrahydroxy-3′-geranyldihydrochalcone.

Compound **4** was obtained as an orange-yellow gum. $[\alpha]_D$ +10° ($CHCl_3$, c 0.08). The UV spectrum exhibited maxima at 224, 279, and 370 nm, and resembled the spectra of a chalcone skeleton. The ^{1}H NMR spectrum of **4** was closely related to that of **1** and showed two sets of ortho-coupled aromatic protons as well as resonances due to a 2-methyl-2-(4-methylpent-3-enyl) 2H-pyran ring. The ^{13}C NMR spectrum of **4** showed 25 resonance signals (**Table 1**). The EIMS of **4** showed the base molecular ion at *m*/*z* 390. From the above results, compound **4** was proposed to be lespeol. The chemical shifts of this compound matched the reported values (*20*).

Compound **5** showed absorption maxima at 228 and 366 nm in the UV spectra. The ^{1}H NMR spectroscopic data of **5** were similar to those of **2**, except for the lack of a singlet aromatic proton and the appearance of an additional ortho-coupled aromatic proton assignable to H-5′ and H-6′, which suggested that the geranyl group was located at C-3′. The ^{13}C NMR spectrum of **5** showed 25 carbon signals (**Table 1**), and the EIMS of **5** exhibited the base molecular ion at *m*/*z* 392 as well as fragment ions at *m*/*z* 323, 269, 203, and 149. From the above results, compound **5** was proposed to be xanthoangelol. The chemical shifts of this compound matched the reported values (*20*).

Effects of Geranyl Chalcone Derivatives on Cell Population Growth and Morphology. To assess whether the five geranyl chalcone derivatives isolated from the leaves of *Artocarpus communis* could inhibit their population growth, SW872, HT-29, COLO 205, Hep3B, PLC5, Huh7, and HepG2 human cancer cells were treated with 0−25 μM of compounds **1**, **2**, **3**, and **5**, and population growth was determined via the MTT assay. The amount of compound **4** isolated from the leaves of *Artocarpus communis* was too low to study the anticancer effects. **Table 2** shows that isolespeol (**1**) had the strongest population growth inhibition of SW 872 human liposarcoma cells among the four geranyl chalcone derivatives tested. Moreover, the 50% inhibitory concentration (IC_{50}) as determined by MTT assay after 48 h of incubation showed the highest activity for isolespeol (**1**), with IC_{50} values of 3.8 μM. Liposarcomas are adipocytic tumors that represent the largest single group of soft tissue tumors (*21*), and the majority are well differentiated. Of cases originally diagnosed between 1972 and 1994, the percentage of soft-tissue sarcomas that were liposarcomas was 21% (*22*). Dei Tos (*23*) indicated that adipocytic liposarcomas are mostly composed of mature adipocytes that exhibit striking variation in cell size. Daugaard (*22*) reported that the soft tissue sarcoma (STS) classification represents a summary of recent pathobiological advances and provides a new baseline for clinical as well as laboratory research. Therefore, isolespeol (**1**) was selected for all subsequent studies. Classical apoptotic cells were identified after isolespeol (**1**) treatment by cell shrinkage, membrane blebbing, and apoptotic body formation (**Figure 3A**). The nuclear morphology of untreated and treated cells is shown in **Figure 3B** and **C** by PI and DAPI staining, respectively. PI and DAPI staining showed apoptotic bodies when cells were treated with 10 μM isolespeol (**1**) for 48 h.

Disruption of Mitochondrial Membrane Potential ($\Delta\Psi$m) by Isolespeol (1). Alterations in mitochondrial function have been shown to play a crucial role in apoptosis; thus, the effect of isolespeol (**1**) on the mitochondrial membrane potential was investigated. In this assay, nonapoptotic cells with healthy mitochondria show red fluorescence, and apoptotic cells show green fluorescence. SW 872 cells showed a significant ($p < 0.05$) decrease in red fluorescence intensity when treated with 0−25 μM isolespeol (**1**) for 6 h (**Figure 4**). Green and Reed (*24*) indicated that the disruption of mitochondrial membrane potential occurs in the early stages of apoptosis, where release of cytochrome *c* from the mitochondria is followed by caspase-3/caspase-9 cascade activation. The present study indicated early damage to the mitochondrial membrane potential that may further activate the intrinsic pathways of apoptosis.

Isolespeol (1) Induces Apoptosis via a Mitochondrial-Mediated Pathway. The Fas (CD95)/Fas Ligand (FasL; CD95L) system is an important extracellular pathway for apoptotic signaling in diverse cell types and tissues (*25*). As shown in **Figure 5**, 10 μM isolespeol (**1**) treatment for 3 h

resulted in significant ($p < 0.05$) 4.98- and 5.38-fold increases in Fas and FasL expression, respectively. Cleavage of Bid by caspase-8 has been reported in many cancer cells undergoing apoptosis induced by Fas and FasL (*26*). Cellular functions modulated by p53 protein include DNA synthesis, DNA repair, gene transcription, cell cycle arrest, and apoptosis. Shen and White (*27*) indicated that expression of the p53 tumor suppressor gene leads either to the induction of cell cycle arrest or to apoptosis. Isolespeol (**1**) treatment at 25 μM for 3 h significantly ($p < 0.05$) stimulated p53 expression by 5.41-fold. The protein expression of Fas, FasL, and p53 did not increase until after 6 h of exposure to isolespeol. The rapid increase in these protein expressions was observed after treatment of isolespeol for 3 h.

Figure 6A shows that treatment with 10 μM isolespeol (**1**) for 3 h significantly ($p < 0.05$) increased Bax expression by 4.92-fold. Treatment at 25 μM for 3 h significantly ($p < 0.05$) decreased Bcl-2 expression to 54% of the control value. Isolespeol (**1**) stimulated Bad and Bid expression in a time- and dose-dependent manner with statistical significance ($p < 0.05$) and maximal increases of 5.08- and 2.47-fold, respectively, after treatment with 10 μM isolespeol (**1**) for 3 h. Isolespeol (**1**) treatment at 10 μM for 6 h significantly ($p < 0.05$) decreased Bcl-X_L expression to 24% of the control value. A significant time- and dose-dependent shift in the ratio of Bax and Bcl-2 expression was observed after isolespeol (**1**) treatment, indicating the induction of apoptotic processes (**Figure 6B**). The ratio of Bax/Bcl-2 plays an important role in determining whether cells undergo apoptosis under experimental conditions that promote cell death (*28*). Madesh et al. (*29*) indicated that the mitochondria undergoing permeability transition cause a loss of mitochondrial membrane potential and cytochrome *c* release in the cytosol. Cory and Adams (*30*) indicated that mitochondrial release of cytochrome *c* can be controlled by the Bcl-2 family of proteins and may be activated by proteolytic cleavage and heterodimerization. Cytochrome *c* release in the cytosolic fraction following isolespeol (**1**) treatment was then investigated. Isolespeol (25 μM, 6 h) resulted in a significant ($p < 0.05$) increase in cytosolic cytochrome *c* expression from 1.00 (control) to 17.6-fold.

Figure 7 shows that exposure of SW 872 cells to isolespeol (**1**) caused the degradation of pro-caspase-8, pro-caspase-9, and pro-caspase-3, which in turn generated caspase-8, caspase-9, and caspase-3 fragments in a time- and dose-dependent manner. Treatment with isolespeol (**1**) also induced cleavage of PARP, which is targeted by active caspase-3 (*31*), in a time- and dose-dependent manner. Tomek et al. (*32*) found TRAIL-induced apoptosis on interaction with cytotoxic agents in soft tissue sarcoma cell lines including rhabdomyosarcoma, fibrosarcoma, liposarcoma, synovial sarcoma, and chondrosarcoma. Our previous study also clearly showed that quercetin induces apoptosis in SW 872 human liposarcoma cells (*33*).

In conclusion, the present study showed that treatment with isolespeol (**1**) led to the loss of mitochondrial transmembrane potential in addition to the regulation of Bcl-2 family members and subsequent activation of caspase-9 and caspase-3, which was, in turn, followed by cleavage of PARP. These results provide a potential molecular mechanism for isolespeol (**1**)-induced apoptosis in SW 872 human liposarcoma cells and suggest that the leaves of *Artocarpus communis* may provide a beneficial effect for human health. Moreover, the cytotoxic effects of other potential compounds from the leaves of *Artocarpus communis* in human cancer cells may also have potential for anticancer applications.

ABBREVIATIONS USED

DAPI, 4, 6-diamidine-2-phenylindole; DMSO, dimethylsulfoxide; IC_{50}, 50% inhibitory concentration; $\Delta\Psi m$, mitochondria membrane potential; MTT, 3-(4,5-dimethylthiazol-2-yl)-2,5-diphenyl tetrazolium bromide; PARP, poly (ADP-ribose) polymerase; PBS, phosphate buffered saline; PI, propidium iodide; PVDF, polyvinyldifluoride; SDS−PAGE, sodium dodecyl sulfate−polyacrylamide gel electrophoresis.

LITERATURE CITED

(1) Vattemi, E.; Claudio, P. P. Tumor suppressor genes as cancer therapeutics. *Drug News Perspect.* **2007**, *20*, 511–520.

(2) Zimmermann, K. C.; Bonzon, C.; Green, D. R. The machinery of programmed cell death. *Pharmacol. Ther.* **2001**, *92*, 57–70.

(3) Johnstone, R. W.; Ruefli, A. A.; Lowe, S. W. Apoptosis: A link between cancer genetics and chemotherapy. *Cell* **2002**, *108*, 153–164.

(4) Vermeulen, K.; Van Bockstaele, D. R.; Berneman, Z. N. Apoptosis: Mechanisms and relevance in cancer. *Ann. Hematol.* **2005**, *84*, 627–639.

(5) Zamzami, N.; Metivier, D.; Kroemer, G. Quantitation of mitochondrial transmembrane potential in cells and in isolated mitochondria. *Methods Enzymol.* **2000**, *322*, 208–213.

(6) Cragg, G. M. Paclitaxel (Taxol): a success story with valuable lessons for natural product drug discovery and development. *Med. Res. Rev.* **1998**, *18*, 315–331.

(7) Zerega, N. J. C.; Ragone, D.; Motley, T. J. Complex origins of breadfruit (*Artocarpus altilis*, Moraceae): implications for human migrations in Oceania. *Am. J. Bot* **2004**, *91*, 760–766.

(8) Kasahara, S.; Hemmi, S. In *Medicinal Herb Index in Indonesia*; P. T. Eisai: Bogor, Indonesia, 1986; p 184.

(9) Fukai, T.; Satoh, K.; Nomura, T.; Sakagami, H. Antinephritis and radical scavenging activity of prenylflavonoids. *Fitoterapia* **2003**, *74*, 720–724.

(10) Shimizu, K.; Kondo, R.; Sakai, K.; Buabarn, S.; Dilokkunanant, U. A geranylated chalcone with 5α-reductase inhibitory properties from *Artocarpus incisus*. *Phytochemistry* **2000**, *54*, 737–739.

(11) Jayasinghe, L.; Balasooriya, B. A. I. S.; Padmini, W. C.; Hara, N.; Fujimoto, Y. Geranyl chalcone derivatives with antifungal and radical scavenging properties from the leaves of *Artocarpus nobilis*. *Phytochemistry* **2004**, *65*, 1287–1290.

(12) Wei, B. L.; Weng, J. R.; Chiu, P. H.; Hung, C. F.; Wang, J. P.; Lin, C. N. Antiinflammatory flavonoids from *Artocarpus heterophyllus* and *Artocarpus communis*. *J. Agric. Food Chem.* **2005**, *53*, 3867–3871.

(13) Han, A. R.; Kang, Y. J.; Windono, T.; Lee, S. K.; Seo, E. K. Prenylated flavonoids from the heartwood of *Artocarpus communis* with inhibitory activity on lipopolysaccharide-induced nitric oxide production. *J. Nat. Prod.* **2006**, *69*, 719–721.

(14) Weng, J. R.; Chan, S. C.; Lu, Y. H.; Lin, H. C.; Ko, H. H.; Lin, C. N. Antiplatelet prenylflavonoids from *Artocarpus communis*. *Phytochemistry* **2006**, *67*, 824–829.

(15) Chan, S. C.; Ko, H. H.; Lin, C. N. New prenylflavonoids from *Artocarpus communis*. *J. Nat. Prod.* **2003**, *66*, 427–430.

(16) Ahi, A. P.; Gonnety, J. T.; Faulet, B. M.; Kouamé, L. P.; Niamké, S. Biochemical characterization of two α-mannosidases from breadfruit (*Artocarpus communis*) seeds. *Afr. J. Biochem. Res* **2007**, *1*, 106–116.

(17) Adewole, S. O.; Ojewole, J. O. Hyperglycaemic effect of *Artocarpus communis* Forst (Moraceae) root bark aqueous extract in Wistar rats. *Cardiovasc. J. Afr* **2007**, *18*, 221–227.

(18) Mosmann, T. Rapid colorimetric assay for cellular growth and survival: application to proliferation and cytotoxicity assays. *J. Immunol. Methods* **1983**, *65*, 55–63.

(19) Mabry, T.; Markham, K. R.; Thomas, M. B. *The Systematic Identification of Flavonoids*; Springer-Verlag: New York, 1970; p 227.

(20) Miyase, T.; Ueno, A.; Noro, T.; Fukushima, S. Studies on the constituents of *Lespedeza cyrtobotrya* Miq. I. The structures of a

new chalcone and two new isoflav-3-ens. *Chem. Pharm. Bull* **1980**, *28*, 1172–1177.
(21) Fletcher, C. D. M.; Unni, K. K.; Mertens, F. 2000. World Health Organization Classification of Tumours. *Pathology and Genetics, Tumours of Soft Tissue and Bone*, 4th ed. IARC Press: Lyon, France.
(22) Daugaard, S. Current soft-tissue sarcoma classifications. *Eur. J. Cancer* **2004**, *40*, 543–548.
(23) Dei Tos, A. P. Liposarcoma: new entities and evolving concepts. *Ann. Diagn. Pathol.* **2000**, *4*, 252–266.
(24) Green, D. R.; Reed, J. C. Mitochondria and apoptosis. *Science* **1998**, *281*, 1309–1312.
(25) Nagata, S.; Golstein, P. The Fas death factor. *Science* **1995**, *267*, 1449–1456.
(26) Li, H.; Zhu, H.; Xu, C.; Yuan, J. Cleavage of BID by Caspase 8 mediates the mitochondrial damage in the Fas pathway of apoptosis. *Cell* **1998**, *94*, 491–501.
(27) Shen, Y.; White, E. p53-Dependent apoptosis pathways. *Adv. Cancer Res.* **2001**, *82*, 55–84.
(28) Merry, D. E.; Korsmeyer, S. J. Bcl-2 gene family in the nervous system. *Annu. Rev. Neurosci.* **1997**, *20*, 245–267.
(29) Madesh, M.; Antonsson, B.; Srinivasula, S. M.; Alnemri, E. S.; Hajnoczky, G. Rapid kinetics of tBid-induced cytochrome c and Smac/ DIABLO release and mitochondrial depolarization. *J. Biol. Chem.* **2002**, *2775651*–5659.
(30) Cory, S.; Adams, J. M. The Bcl-2 family: Regulators of the cellular life-or-death switch. *Nat. Rev. Cancer* **2002**, *2*, 647–656.
(31) Debatin, K. M.; Krammer, P. H. Death receptors in chemotherapy and cancer. *Oncogene* **2004**, *23*, 2950–2966.
(32) Tomek, S.; Koestler, W.; Horak, P.; Grunt, T.; Brodowicz, T.; Pribill, I.; Halaschek, J.; Haller, G.; Wiltschke, C.; Zielinski, C. C.; Krainer, M. Trail-induced apoptosis and interaction with cytotoxic agents in soft tissue sarcoma cell lines. *Eur. J. Cancer* **2003**, *39*, 1318–1329.
(33) Huang, S. H.; Hsu, C. L.; Yen, G. C. Growth inhibitory effect of quercetin on SW 872 human liposarcoma cells. *Life Sci.* **2006**, *79*, 203–209.

Received for review June 6, 2008. Revised manuscript received August 6, 2008. Accepted August 6, 2008. This research work was partially supported by the National Science Council, the Republic of China, under grant NSC96-2321-B005-002.

JF8017436